Characterization of two-color ultrashort laser pulses using polarization-gating and transient-grating frequency-resolved optical gating

Soroush D. Khosravi,[1,*] Rana Jafari,[2,3] Mark Schittenhelm,[1] Sadhana Suresh,[4] George N. Gibson,[4] and Rick Trebino[2]

[1]*Mathematics & Physics Department, Queens University of Charlotte, 1900 Selwyn Ave., Charlotte, North Carolina 28274, USA*
[2]*School of Physics, Georgia Institute of Technology, 837 State St. NW, Atlanta, Georgia 30332, USA*
[3]*Swamp Optics LLC, 6300 Powers Ferry Road, Suite 600-345, Atlanta, Georgia 30339, USA*
[4]*Department of Physics, University of Connecticut, 196A Auditorium Road, Unit 3046, Storrs, Connecticut 06269, USA*
Corresponding author: khosravis@queens.edu

Two-color ultrashort laser pulses have emerging applications in numerous areas of science and technology. In many cases, the slightest change in the combined electric field of a two-color pulse greatly affects its interaction mechanism with the system. Therefore, a precise characterization of the temporal/spectral profile of the combined electric field is of great importance. In this work, we demonstrate that a full characterization is possible using the well-known transient-grating (TG) or polarization-gating (PG) frequency-resolved optical gating (FROG) techniques, and by employing the recently developed Retrieved-Amplitude N-grid Algorithmic (RANA) approach for the retrieval process. We demonstrate the validity of using these techniques and this approach for multi-cycle and few-cycle pulses in the absence and presence of noise. © 2022 Optica Publishing Group

1. INTRODUCTION

An ultrashort two-color (or bichromatic) laser pulse is composed of two individual pulses (termed as components) with different center frequencies, which propagate collinearly in a medium. The two components might have distinct amplitudes, absolute phases, and chirps. Also, there could be a temporal separation between them. These parameters determine the combined electric field of the two-color pulse, which ultimately governs the nature of its interaction with matter. Therefore, full and precise knowledge of the temporal/spectral profile of the combined electric field at the time of interaction with matter is of great importance. To fully describe such a two-color laser pulse requires knowledge of its intensity and phase versus time or, equivalently, its spectrum and spectral phase, which contain all the information about the two components' electric field's relative amplitude, relative phase, temporal separation, and any other higher-order dispersion.

Two-color pulses have applications across many fields, including the development of novel table-top light sources, the implementation of various spectroscopic techniques, and quantum control. Interaction of intense ultrashort laser pulses, normally in the infrared or visible spectral regions, with matter can lead to the generation of harmonics in the extreme

ultraviolet and soft x-ray regions. This strong-field nonlinear process is called high-order harmonic generation (HHG) and is promising for the development of future table-top coherent light sources with attosecond pulse duration [1–3]. A single ultrashort laser pulse is commonly used for the HHG process. However, utilizing a two-color laser pulse has been suggested due to the additional control and advantages it can provide for an optimal HHG process. This has been investigated extensively both experimentally [4–7] and theoretically [8–10], and promising results have been reported. Some of the reported advantages include (1) enhancement of harmonic intensity yield, (2) extension of the cutoff frequency, (3) improvement of the temporal profile of the harmonics and HHG spectrum, (4) control over the electron trajectories and relative yield of odd and even harmonics, and (5) the realization of isolated attosecond pulses [11–19]. These enhancements can be achieved by adjusting the amplitude ratio, the temporal separation, the relative phase, and/or the linear chirp of the components of the interacting two-color laser pulse.

Spectral broadening of ultrashort laser pulses when propagating through a transparent nonlinear medium, such as sapphire or optical fiber, results in the generation of a highly coherent

broadband light, called supercontinuum (or white-light continuum, WLC). Supercontinua in the visible and infrared regions are widely used as probe pulses in various time-resolved spectroscopic techniques [20], as the seed pulse in different optical parametric amplifiers (OPAs) [21], and as the light source in many other applications. Using a two-color laser pulse instead of a single laser pulse to generate the supercontinuum is investigated and is proven to be an effective method to optimize the generation mechanism. The improvement of the supercontinuum spectra [22–24] and the enhancement of the conversion efficiency [25–27] are reported by adjusting the relative amplitude or phase of the driving two-color field.

Ultrashort terahertz radiation generation, in the spectral region between infrared and microwave, has been studied for the past two decades, and extensive research is underway to achieve more powerful terahertz radiation sources [28–30]. Such powerful sources would enable nonlinear terahertz science and many other fascinating applications [31]. One of the most promising methods for the development of powerful and efficient terahertz radiation sources involves the use of two-color pulses as the driving field [32–35]. High energy single-cycle terahertz radiation have been recently realized by employing mid-infrared two-color pulses in ambient air [34]. It has been shown that the efficiency of terahertz radiation generation strongly depends on the relative phase of the driving two-color pulse [33].

Another class of two-color pulse applications is the higher-level control of ultrafast dynamics in atomic and molecular systems by employing such pulses for excitation, ionization, or dissociation. It has recently been demonstrated that the angular distribution of photoelectrons in the strong-field single ionization of argon atoms can be rotated in the polarization plane by adjusting the relative phase of the interacting two-color field [36]. The photoelectron momentum distribution has also been shown to be affected by adjusting the relative phase. It was concluded that the Coulomb effect on the evolution of the tunneling electron wave packet strongly depends on the combined electric field of the driving two-color pulse [37]. It was also suggested that monitoring the photoelectron momentum distribution as a function of the relative phase would enable the retrieval of electron trajectories and ionization times [38]. Furthermore, adjusting the amplitude ratio was shown to affect the orientation-dependent ionization rates of molecules like H_2O and S_2O, and it was suggested as a possible means for molecular orbital imaging [39]. More recently, it has been shown that manipulation of the combined electric field of an interacting two-color pulse can lead to the generation of complex light-induced molecular potentials (LIPs) and canonical intersections (LICIs), which ultimately regulate the outcome of molecular dissociation processes [40,41]. Lastly, coherent control of above-threshold photoemission from a metallic nanotip has been reported and strong dependence of electron emission on the temporal separation between the components of the driving two-color pulse was observed [42]. Ultrashort two-color laser pulses can be utilized in many other similar quantum control experiments [43–47], as well as in other ultrafast science applications.

In all these applications, the precise and complete characterization of the driving two-color electric field is crucial because it governs the interaction and ultimately the outcome of the experiment. For example, a precise real-time characterization of the interacting pulse would facilitate the manipulation of the HHG process, and eventually the engineering of an optimal table-top coherent light source. Also, in terahertz applications, a full characterization of the driving pulse would enable one to monitor and isolate the influencing parameters and move towards the realization of terahertz radiation sources in the nonlinear energy regime. Unfortunately, the complete intensity and phase measurement of such two-color ultrashort waveforms has proven challenging for all measurement techniques. Specifically, there are ambiguities in the relative phases of well-separated pulses. While the polarization gating (PG) and transient grating (TG) versions of the frequency-resolved optical gating (FROG) [48] are able to measure such phases, the second-harmonic generation (SHG) version of FROG has a one-parameter ambiguity: if its algorithm returns a relative phase of φ, then the value $\varphi + \pi$ is also possible. When measuring simple spectrograms (also known as XFROG traces) of such pulses, the relative phase of the pulses cannot be measured at all. Well-separated modes in frequency are even more problematic. Keusters *et al.* showed that their relative phases are simply not measurable at all using most techniques, including FROG [49].

However, when some temporal overlap occurs between two pulses or when some spectral overlap occurs between two modes in the waveform, the relative phase becomes measurable. But, if the overlap is minimal, there remains an "approximate ambiguity" in the sense that the wrong phase yields a retrieved trace that is very similar to the correct trace. In the presence of noise, the measurement could easily become ambiguous again. Even in the absence of noise, any pulse-retrieval algorithm could become confused and stagnate on the wrong phase value. As a result, waveforms with slightly overlapping pulses or modes are not only important but also prove to be an excellent test for pulse-measurement techniques and their algorithms.

Algorithm stagnation has long been an issue in pulse-measurement techniques. Even FROG's standard generalized projections (GP) algorithm [50,51], which works very well for relatively simple pulses, tends to stagnate for more complex pulses [52]. Other proposed algorithms address other issues, such as speed, ease of programming, or missing data, but do not improve convergence. Recently, however, a much more robust FROG pulse-retrieval algorithmic approach, called the Retrieved-Amplitude N-grid Algorithmic (RANA) approach, was introduced for common FROG variations [53–55].

The RANA approach works by first *directly* retrieving the spectrum from the FROG trace without additional measurements and using it as the initial guess for the algorithm. Second, a set of a dozen or so initial guesses are generated, all with the directly retrieved spectrum but with random noise for the spectral phase. Third, these initial guesses are then quickly run on smaller, coarser grids generated from the full trace [56,57], removing the poorly performing pulses and keeping only the best-performing ones.

The RANA approach is very general, and it works in conjunction with any FROG algorithm. When incorporating the well-known standard GP algorithm, the RANA approach achieved convergence for 100.00% of tens of thousands of even extremely complex noise-like simulated pulses with time–bandwidth products (TBPs) as high as 100 and also in

the presence of significant noise in the measured trace. It has also successfully retrieved measured pulses that have confused the standard GP algorithm [58]. We believe that the RANA approach is an important development, but it has not, however, been tested for waveforms with only slightly overlapping pulses or modes. As these two-color waveforms are particularly important and challenging, it is important to test the RANA approach on them and to compare its performance for them with the standard GP algorithm.

In this work, we examine the reliability of the PG/TG FROG version of the RANA approach for the full characterization of multi-cycle and few-cycle two-color ultrashort laser pulses having varying degrees of spectral overlap between the components. We investigate the retrieval quality for different values of all of the above-mentioned parameters relevant in common experimental settings.

2. SIMULATIONS AND RETRIEVAL ALGORITHMS

The schematics of PG and TG FROG instruments are shown in Fig. 1. In a PG FROG instrument, a replica of the two-color pulse is used as the gate and is incrementally delayed with respect to the probe pulse. The nonlinear optical interaction of the gate and the probe pulses in the medium generates a delay-dependent signal pulse, which is then spectrally resolved by a spectrometer. The resulting spectrally resolved signal versus delay forms a FROG trace on the camera. As mentioned in [59], TG FROG traces are mathematically equivalent to PG FROG traces if the time delay is applied to the probe pulse and there is no delay between the excitation pulses, as shown on the bottom panel of Fig. 1. Both PG and TG FROG instruments work well and are in common use worldwide, although experimental TG

FROG traces typically have a better signal-to-noise ratio compared to PG FROG traces due to their mostly background-free detection.
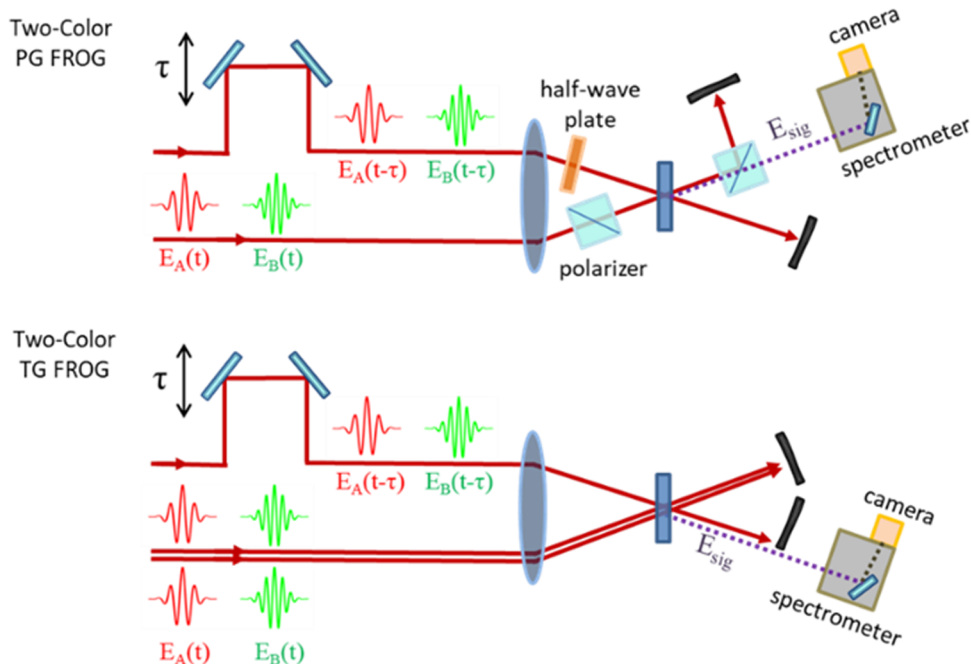
A modified version of the MATLAB script described in our recent paper [45], was used to simulate the two-color FROG traces. The traces are constructed using the discrete version of the following equation. Next, the generated simulated traces (non-square arrays) were interpolated to generate smaller $N \times N$ traces for the phase retrieval. As seen in the equation below, the gate and the probe electric fields are both the combined temporal electric field of the two-color pulse. We have

$$I_{\mathrm{FROG}}^{\mathrm{PG/TG}}(\omega, \tau) = \left| \int_{-\infty}^{+\infty} [E_A(t \pm \tau) + E_B(t \pm \tau)] \right.$$

$$\times \left. |[E_A(t) + E_B(t)]|^2 e^{-i\omega t} \mathrm{d}t \right|^2,$$

where t is time, τ is the delay, and ω is the angular frequency.

Different orders of dispersion, i.e., the absolute phase (φ_0), the temporal separation (φ_1), the linear chirp (φ_2), and the third-order dispersion (TOD) (φ_3), were added to each individual pulse A or B in the simulation script where the spectral phases of pulse A or B are defined using the following equation. The term "relative phase" throughout the article represents the absolute phase difference between pulse A and B (i.e., $\Delta\varphi_0 = \varphi_{0B} - \varphi_{0A}$) and should not be confused with the overall phase difference (i.e., $\Delta\varphi = \varphi_B - \varphi_A$).

$$\varphi_{A/B} = \varphi_{0A/B} + \varphi_{1A/B}(\omega - w_{0A/B}) + \frac{1}{2!}\varphi_{2A/B}(\omega - w_{0A/B})^2$$

$$+ \frac{1}{3!}\varphi_{3A/B}(\omega - w_{0A/B})^3.$$

Fig. 1. Schematic of the two-color PG and TG FROG instruments. A two-color pulse and its replica are used as the gate and the probe in the FROG instruments.

Three regimes were investigated throughout this work where the two components of the pulse are (1) well separated ($f_{0A} = 375$ THz, $f_{0B} = 438$ THz), (2) partially overlapped ($f_{0A} = 375$ THz, $f_{0B} = 414$ THz), or (3) strongly overlapped ($f_{0A} = 375$ THz, $f_{0B} = 392$ THz) in the frequency domain. A pulse duration of 40 fs was considered for each component in all cases except for the few-cycle pulses. The components were given the same amplitude. Additive noise was applied using a Poisson distribution for the noise dependence investigations. The PG RANA approach [53–55] was used for all the retrievals. The GP algorithm [50] was used in section 3.F to compare its retrieval effectiveness with that of the RANA approach.

3. RESULTS AND DISCUSSION

We investigated the retrieval of two-color ultrashort laser pulses from PG or TG FROG traces using the RANA approach. First, we should point out that all the FROG traces studied here were distinct. In other words, they did not reveal any new ambiguities beyond the well-known case of the pulses with well-separated components whose different relative phases are not retrievable (the well-separated modes' relative phase ambiguity) and which is discussed in subsection 3.A. Our retrieval results for pulses with zeroth- up to third-order dispersion (i.e., relative phase, temporal separation, linear chirp, or TOD) are discussed separately in the following subsections. We also examined the applicability of these techniques for the characterization of two-color few-cycle pulses and the retrieval from noisy FROG traces, which are discussed in subsections 3.D and 3.E, respectively. Employment of the RANA approach led to rapid convergence, accurate retrieval, and negligible residual trace error for all the FROG traces studied in this work. Lastly, we find that the standard GP algorithm exhibits weaker performance than does the RANA approach for the retrieval of two-color FROG traces. The standard GP algorithm is slower for most traces and even failed to converge for some of the more complex traces, as demonstrated in subsection 3.F.
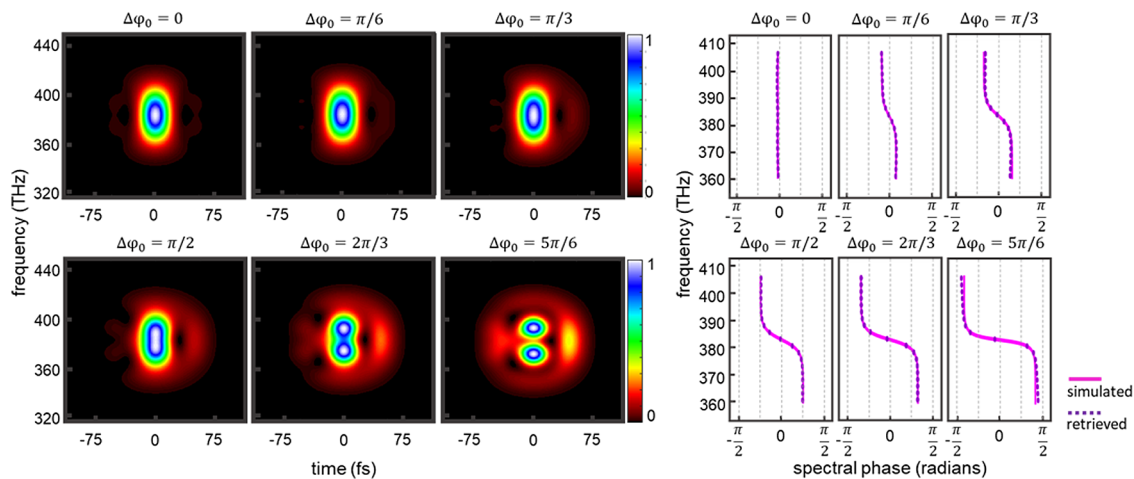
A. Relative Phase

As mentioned above, when the components of a two-color laser pulse are well separated in frequency, most techniques, including PG and TG FROG, cannot measure the relative phase ($\Delta\varphi_0$) between the two components. As seen in the first column of Fig. 2, all FROG traces of such pulses are identical, regardless of their different values of relative phase.

The FROG traces are distinct and depend on their relative phase values when the two components are partially or strongly overlapped in frequency (second and third columns of Fig. 2). In such cases, the relative phase between the two components of the pulse is retrievable using the RANA approach. The phase retrieval results are shown in the right panel of Fig. 3 for the case of the strongly overlapped components. The retrieved spectral phases agree with the simulated ones for different values of the relative phases ($\Delta\varphi_0 = 0, \pi/6, \ldots, 5\pi/6$).

This demonstrates that the relative phase between two unknown colinearly propagating ultrashort laser pulses can
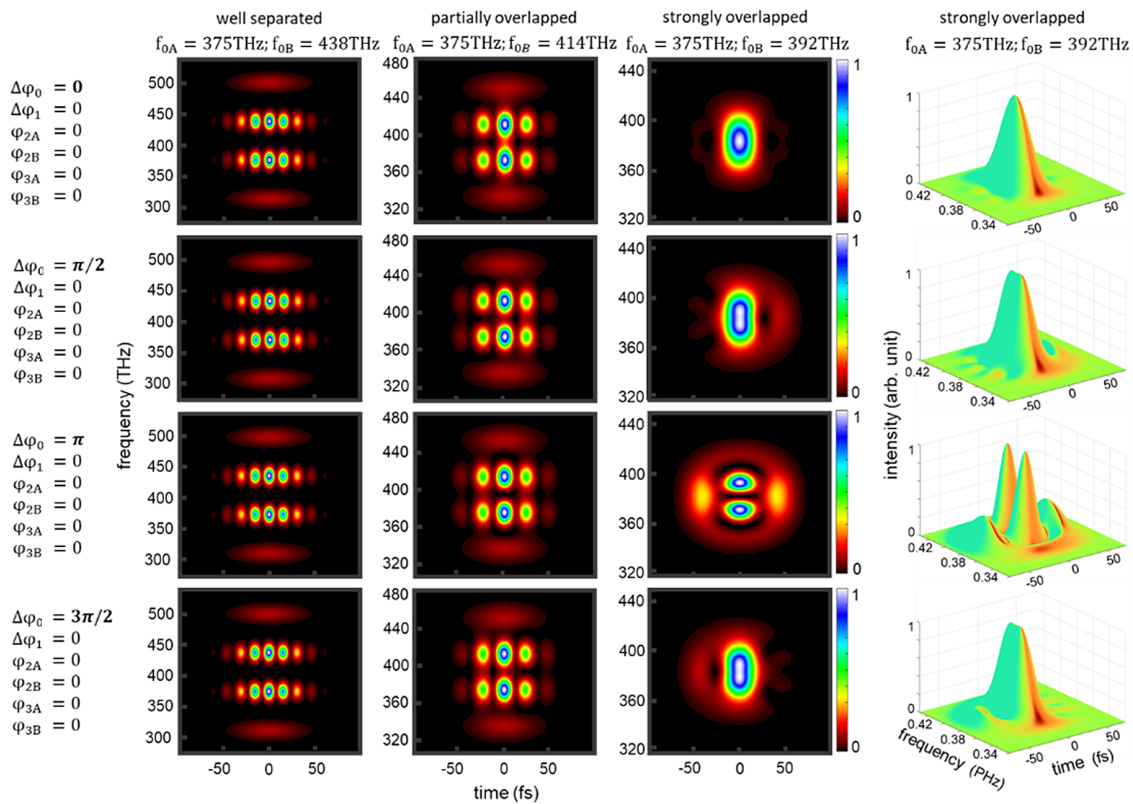
Fig. 2. Simulated PG/TG FROG traces with different values of relative phase between the component of a two-color ultrashort laser pulse. The components of the pulse have the same amplitudes and pulse durations (40 fs). Three-dimensional plots for the case of strongly overlapped components are shown in the fourth column for a better visualization of the spectro-temporal intensity profile.

Fig. 3. Retrieval of the relative phase between two components of a two-color laser pulse using the RANA approach. In the plots, because the spectral phase is meaningless when the spectral intensity is zero, the spectral phase values are zeroed at intensity levels below 0.5% of the maximum intensity.

be measured directly using a PG or TG FROG instrument and employing the RANA approach for pulse-retrieval. Such measurements can be conducted using single-shot FROG instruments (or multi-shot FROG if the pulses are relative-phase stabilized). For a better visualization of the spectro-temporal intensity profile, three-dimensional plots of the FROG traces are shown for the case of strongly overlapped components in the fourth column of Fig. 2.

B. Temporal Separation between the Two Components

In many applications, the precise measurement and control of the temporal separation between the components of a two-color laser pulse are required in order to regulate the outcome of its interaction with the system. The temporal separation between the two components is readily measurable using PG or TG FROG traces if it is large enough compared to the pulse duration (last row of Fig. 4). In such cases, the temporal separation between either of the two side lobes and the center lobe of the FROG trace represents the separation between the two components. Furthermore, for two-color pulses with strongly overlapped components (right bottom trace in the figure), the fringe spacing along the frequency axis in the center lobe corresponds to the temporal separation between the two components (temporal separation in fs = 1/fringe spacing in PHz). But the temporal separation is not readily measurable if it is comparable to the pulse duration (second and third rows in Fig. 4), depending on the strengths of the modes' spectral wings. Measuring the separation in this small-separation regime and realizing the zero-separation instance are of great importance in various applications, e.g., [10,13,24]. So we examined the applicability of the RANA approach to achieve this goal.

We tested all traces shown in Fig. 4 and found that the RANA approach retrieves the precise temporal separation between the components of a two-color ultrashort laser pulse. This is true for any arbitrary separation, including the zero-, small-, and large-separation regimes. The retrieval results are shown for two-color pulses with 40 fs or 41.7 fs separations on the top panel

of Fig. 5. After the retrieval process, the separations between the two components are simply determined using the slope of the retrieved spectral phase (rad) versus the angular frequency (rad/s) graph for regions where the intensity is non-zero. This provides a powerful tool for measuring the precise separation between the components of ultrashort two-color laser pulses (for the compressed pulses for which the higher-order spectral phase is removed).

It should be noted that even a small change in the temporal separation between the two components (a change of around 1.7 fs when the optical cycle is approximately 2.6 fs) can dramatically alter the combined electric field of the interacting two-color pulse, as shown on the bottom panel of Fig. 5 (C and D). In this figure, the intensity of the combined electric field is shown in orange, and its amplitude is shown in yellow. The optical cycles are not distinguishable due to the low resolution of the figure. The dramatic change in the combined electric field is due to the destructive or constructive interferences between the electric fields of the two components. This indicates the importance of precisely controlling the temporal separation in single-shot experiments involving two-color laser pulses in order to obtain reproducible results. The respective FROG traces for such cases are clearly distinct, and the RANA approach is able to retrieve the precise spectral phase and temporal separation.

C. Dependence on Linear Chirp and Third-Order Dispersion

Chirped two-color pulses can be utilized in different light generation applications or molecular excitation schemes [14,45], and their full characterization is desired. In this section, we show that such pulses having second-order (linear chirp) or third-order dispersion are reliably retrievable using the RANA approach. FROG traces, as well as their retrieved spectra and spectral phases, are shown in Fig. 6.

As seen, the retrieved spectra and spectral phases for all cases agree well with the simulated ones, even for highly complex FROG traces. As expected, the fringe spacing along the
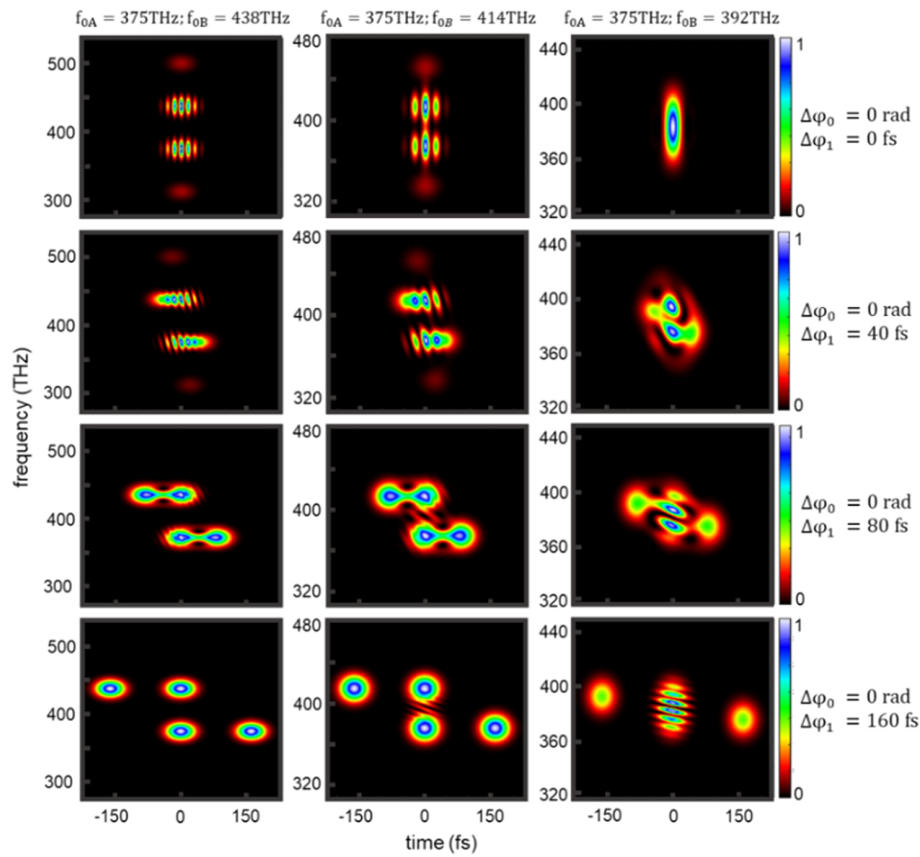
Fig. 4. Simulated PG/TG FROG traces with different temporal separations between the components of a two-color pulse. The zero-, small-, and large- temporal separation regimes are compared.
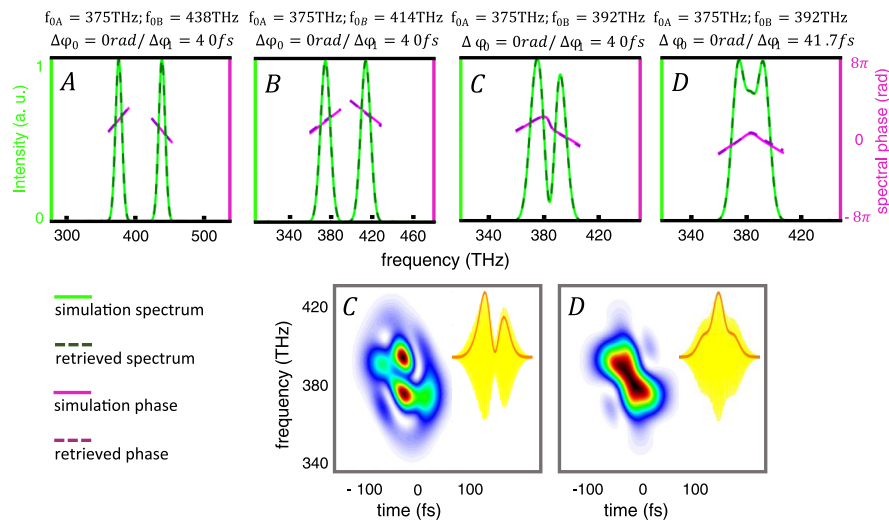

Fig. 5. Retrieval of the temporal separation between the components of a two-color pulse with a 40 fs or 41.7 fs separation between the components. The FROG trace and combined electric field (orange line) alter dramatically with a small change (1.7 fs) in the temporal separation between the components.

time-delay axis for the case where both components have positive (second column of the figure) or negative linear chirp corresponds inversely to the difference in the center frequency of the two components (fringe spacing = 1/center frequency difference).

D. Retrieval of Few-Cycle Pulses

The applicability of the RANA approach is not limited to multicycle pulses. In this section, we demonstrate that the RANA approach can also be employed to fully characterize few-cycle
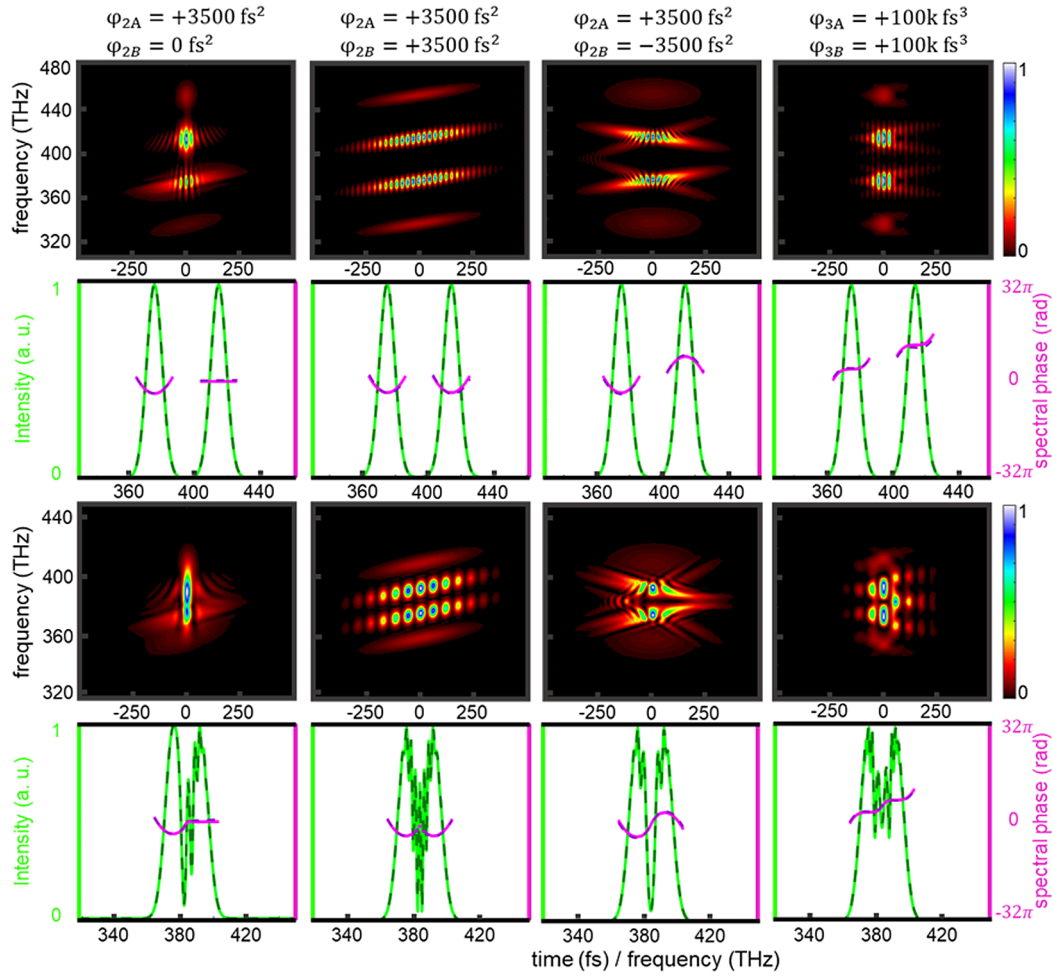
Fig. 6. Retrieved spectra and spectral phases of two-color laser pulses having linear chirp or third-order dispersion, and their respective PG/TG FROG traces. The top panel shows the results for two-color pulses with partially overlapping components ($f_{0A} = 375$ THz, $f_{0B} = 414$ THz). The bottom panel shows the results for two-color pulses with strongly overlapping components ($f_{0A} = 375$ THz, $f_{0B} = 392$ THz).

pulses. Specifically, we show that the relative phase ($\Delta\varphi_0$) between two unknown, collinearly propagating, few-cycle pulses can be directly measured using a single-shot PG or TG FROG and by employing the RANA approach for the retrieval process.

The retrieval results for a two-color few-cycle pulse having a 2.5 fs component centered at 600 nm and a 4 fs component centered at 1200 nm, are shown in Fig. 7. Different values of the relative phase ($\Delta\varphi_0$) and the temporal separation ($\Delta\varphi_1$) were studied. The respective FROG traces for each case are shown in the inset. The intensity of the combined electric field (orange line), and the amplitude of the electric field of each component (blue and yellow lines) are depicted in separate cells. The results in the top two panels of the figure indicate that the relative phase is precisely retrievable for all the cases, including the zero relative phase. As is evident, the intensity profile of the combined electric field of a two-color pulse alters dramatically by changing the relative phase. This explains the strong dependence on the relative phase observed in different experiments.

The retrieval results for cases with zero relative phase and non–zero temporal separation are shown on the bottom two panels of the figure. As is evident, the spectra and spectral phases

are retrievable for such cases, and consequently, the temporal separation between the two components can be calculated as explained in subsection 3.B. Cases with a linear chirp or a combination of different orders of dispersion were also studied and are all retrievable. They are not included in this figure for brevity.

### E. Effect of Noise on Retrieval Quality

The presence of noise in the PG/TG FROG traces necessarily affects the retrieval quality. The retrieved spectra and phases are compared for FROG traces with 0% or 2% additive noise in the left panel of Fig. 8. These results are obtained for an extreme case when the multi-cycle, two-color pulse has a combination of zeroth- to third-order dispersion ($\Delta\varphi_0 = \frac{\pi}{2}$ rad, $\Delta\varphi_1 = 120$ fs, $\varphi_{2A} = \varphi_{2B} = 1500$ fs^2, and $\varphi_{3A} = \varphi_{3B} = 5k$ fs^3) and the components of the pulse are strongly overlapped in the frequency domain. The G-Error (rms difference between the simulated and retrieved traces) is only around 0.0031 with 2% additive noise. The dependence of the G-Error on the noise level for other values of additive noise is shown in the right panel of the figure. The uncertainty values in the figure are obtained by calculating the standard deviation of 10 retrieval trials for
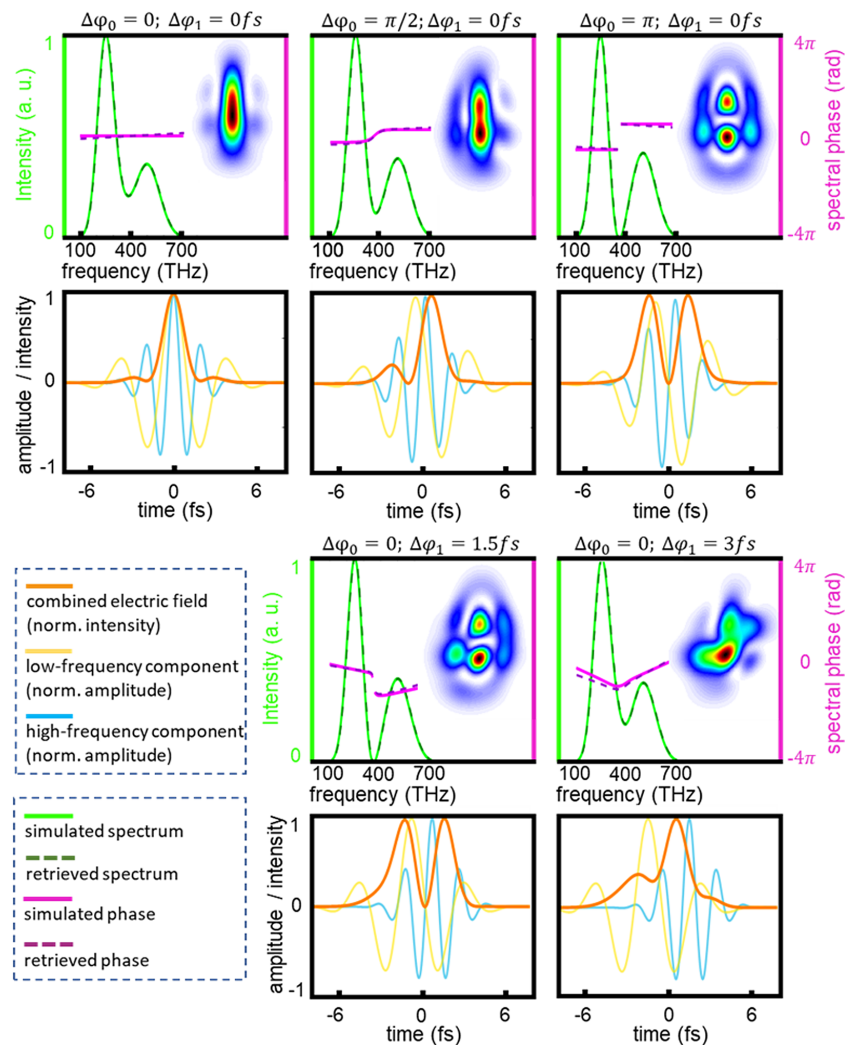
Fig. 7.   Direct retrieval of the relative phase ($\Delta\varphi_0$) and the temporal separation ($\Delta\varphi_1$) between two unknown, colinearly propagating, few-cycle pulses using the RANA approach.
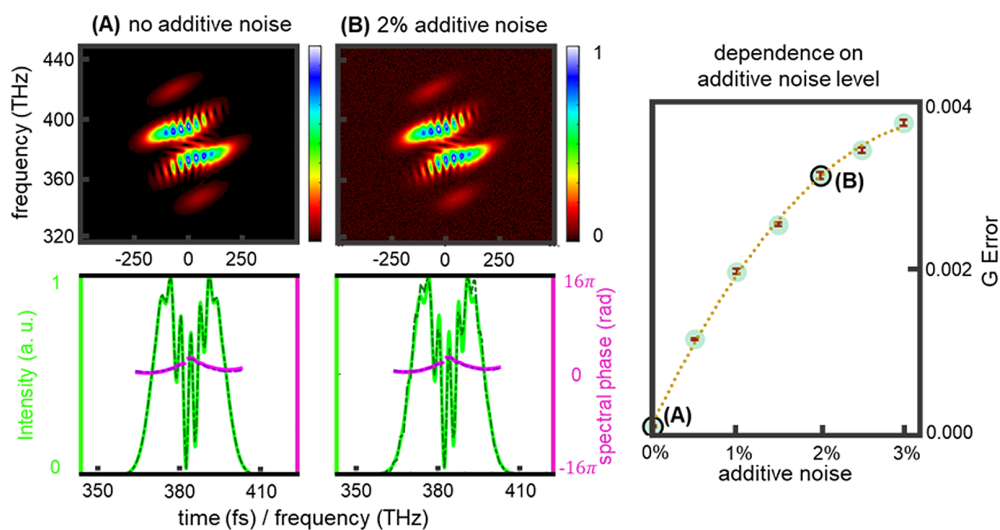
Fig. 8.   Effect of noise contamination on the retrieval quality for a complex two-color pulse having a combination of zeroth to third-order dispersion. The dependence of G-Error (rms difference between the simulated and retrieved traces) on the additive noise level is shown in the right panel.
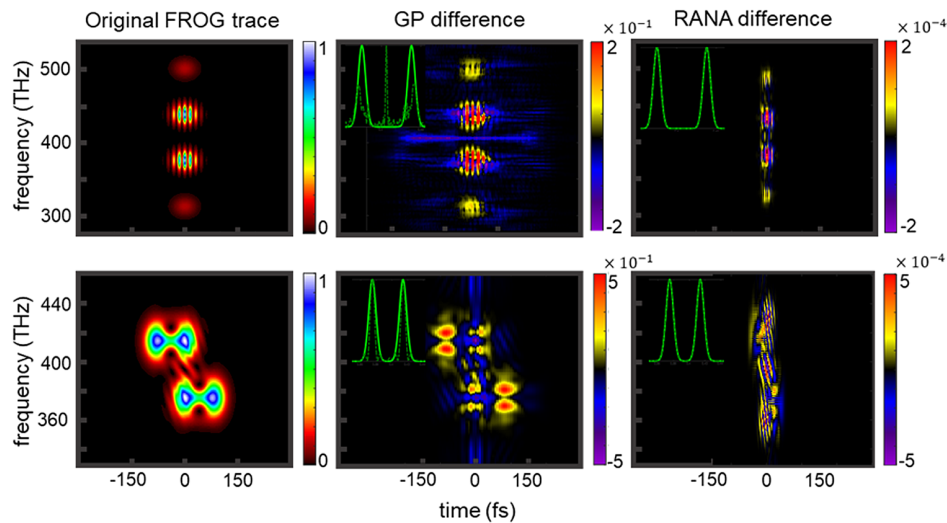
Fig. 9. Comparison of the retrieval of two-color pulses using the standard GP algorithm and the RANA approach. The standard GP fails to converge for complex traces. But the RANA approach reliably and rapidly retrieves the two-color FROG traces.

each additive noise value. These results and the small values of the standard deviations indicate the robustness of the RANA approach for the retrieval of two-color pulses in the presence of noise.

F. Comparison of GP and RANA Approaches

The standard GP algorithm has a weaker performance than the RANA approach for the retrieval of two-color FROG traces. The standard GP algorithm is slower for most traces, and it does not even converge for some of the more complex traces. Two of the cases where the GP algorithm does not converge and therefore is unable to retrieve the spectra are shown in Fig. 9. As is evident, the difference (residual) matrix is much larger when the GP algorithm is used. Also, the retrieved spectra, shown in the inset of the figure, do not agree with the simulated ones, whereas these problems do not occur with the RANA approach.

4. CONCLUSION AND FUTURE WORK

We demonstrate that a two-color ultrashort laser pulse can be fully characterized (up to the inherent ambiguities) using PG or TG FROG instruments and by employing the RANA approach for the retrieval process. This is valid regardless of the center-frequencies of the two components of the pulse or the degree of their spectral overlap. The retrieval provides information about relative amplitude, relative phase, temporal separation, linear chirp, and third-order dispersion, which are needed to control and optimize the interaction of such pulses with systems of interest. The only limitation is the well-known ambiguity of the relative phase for the case of two-color pulses with well-separated components in the frequency domain. In such cases, the FROG traces are entirely identical for different values of the relative phase, as is known. This is because there is no frequency-overlap to cause interference, which would contain the relative phase information. Indeed, no relative phase information exists in the FROG trace to be retrieved by the algorithm. We also show that a small change, comparable to the

optical cycle period, in the temporal separation between the two components can dramatically alter the combined electric field of the two-color pulse. Therefore, precise control of the temporal separation between the two components would be necessary to obtain reproducible results in single-shot experiments involving two-color pulses.

Furthermore, we demonstrate the importance of the RANA approach for the characterization of few-cycle two-color pulses. Specifically, we show that the relative phase between two colinearly propagating, few-cycle pulses can be directly measured using this approach. The only requirement is a partial overlap in frequency, which is easily achievable due to the large bandwidth of such pulses. Indeed, a pulse that has finite temporal support necessarily has infinite spectral support (or extent). We also show that the RANA approach remains robust in the presence of noise and also when a combination of different orders of dispersion are applied to the two-color laser pulse.

PG and TG FROG instruments are widely used in ultrafast science laboratories. This work shows that two-color laser pulses can simply be characterized using available FROG setups with no need for alterations or additional equipment when the RANA approach is used for the retrieval process. The only requirement is that the entire bandwidth of the two-color pulse is supported by the optical elements in the FROG instrument. SHG FROG is another common ultrashort pulse characterization device, and we plan to investigate its capabilities for the characterization of ultrashort two-color laser pulses in future work.

REFERENCES

1. S. Chatziathanasiou, S. Kahaly, E. Skantzakis, G. Sansone, R. Lopez-Martens, S. Haessler, K. Varju, G. D. Tsakiris, D. Charalambidis, and P. Tzallas, "Generation of attosecond light pulses from gas and solid state media," Photonics **4**, 26 (2017).

2. S. Ghimire and D. A. Reis, "High-harmonic generation from solids," Nat. Phys. **15**, 10–16 (2019).

3. J. Li, J. Lu, A. Chew, S. Han, J. Li, Y. Wu, H. Wang, S. Ghimire, and Z. Chang, "Attosecond science based on high harmonic generation from gases and solids," Nat. Commun. **11**, 2748 (2020).

4. M. D. Perry and J. K. Crane, "High-order harmonic emission from mixed fields," Phys. Rev. A **48**, R4051–R4054 (1993).

5. S. Watanabe, K. Kondo, Y. Nabekawa, A. Sagisaka, and Y. Kobayashi, "Two-color phase control in tunneling ionization and harmonic generation by a strong laser field and its third harmonic," Phys. Rev. Lett. **73**, 2692–2695 (1994).

6. R. A. Ganeev, M. Suzuki, and H. Kuroda, "Enhanced harmonic generation using different second-harmonic sources for the two-color pump of extended laser-produced plasmas," J. Opt. Soc. Am. B **31**, 911–918 (2014).

7. G. S. Boltaev, M. Iqbal, N. A. Abbasi, V. V. Kim, R. A. Ganeev, and A. S. Alnaser, "Enhanced XUV harmonics generation from diatomic gases using two orthogonally polarized laser fields," Sci. Rep. **11**, 5534 (2021).

8. A. D. Bandrauk, S. Chelkowski, H. Yu, and E. Constant, "Enhanced harmonic generation in extended molecular systems by two-color excitation," Phys. Rev. A **56**, R2537–R2540 (1997).

9. C. Jin, G. Wang, A.-T. Le, and C. D. Lin, "Route to optimal generation of soft x-ray high harmonics with synthesized two-color laser pulses," Sci. Rep. **4**, 7067 (2014).

10. F. Navarrete and U. Thumm, "Two-color-driven enhanced high-order harmonic generation in solids," Phys. Rev. A **102**, 063123 (2020).

11. D. B. Milosević and W. Sandner, "Extreme-ultraviolet harmonic generation near 13 nm with a two-color elliptically polarized laser field," Opt. Lett. **25**, 1532–1534 (2000).

12. D. Peng, L.-W. Pi, M. V. Frolov, and A. F. Starace, "Enhancing high-order-harmonic generation by time delays between two-color, few-cycle pulses," Phys. Rev. A **95**, 033413 (2017).

13. P. Matía-Hernando, T. Witting, D. J. Walke, J. P. Marangos, and J. W. G. Tisch, "Enhanced attosecond pulse generation in the vacuum ultraviolet using a two-colour driving field for high harmonic generation," J. Mod. Opt. **65**, 737–744 (2018).

14. M. Mofared, E. Irani, and R. Sadighi-Bonabi, "Enhancing high harmonic generation by the global optimization of a two-color chirped laser field," Phys. Chem. Chem. Phys. **21**, 9302–9309 (2019).

15. R. A. Ganeev, C. Hutchison, A. Zaïr, T. Witting, F. Frank, W. A. Okell, J. W. G. Tisch, and J. P. Marangos, "Enhancement of high harmonics from plasmas using two-color pump and chirp variation of 1 kHz Ti:sapphire laser pulses," Opt. Express **20**, 90–100 (2012).

16. L. He, G. Yuan, K. Wang, W. Hua, C. Yu, and C. Jin, "Optimization of temporal gate by two-color chirped lasers for the generation of isolated attosecond pulse in soft x rays," Photon. Res. **7**, 1407–1415 (2019).

17. Y. Wang, H. Wu, Y. Qian, Q. Shi, C. Yu, Y. Chen, K. Deng, and R. Lu, "Laser-parameter effects on the generation of ultrabroad harmonic and ultrashort attosecond pulse in a long-plus-short scheme," J. Mod. Opt. **59**, 1640–1649 (2012).

18. C. Hutchison, S. Houver, N. Lin, D. J. Hoffmann, F. McGrath, T. Siegel, D. R. Austin, A. Zaïr, P. Salières, and J. P. Marangos, "Electron trajectory control of odd and even order harmonics in high harmonic generation using an orthogonally polarised second harmonic field," J. Mod. Opt. **61**, 608–614 (2014).

19. G. Zhang, "Generation of an extreme ultraviolet supercontinuum in a two-color spatially inhomogeneous field," J. Mod. Opt. **62**, 1515–1526 (2015).

20. M. Maiuri, M. Garavelli, and G. Cerullo, "Ultrafast spectroscopy: state of the art and open challenges," J. Am. Chem. Soc. **142**, 3–15 (2020).

21. C. Manzoni and G. Cerullo, "Design criteria for ultrafast optical parametric amplifiers," J. Opt. **18**, 103501 (2016).

22. K. Wang, L. Qian, H. Luo, P. Yuan, and H. Zhu, "Ultrabroad supercontinuum generation by femtosecond dual-wavelength pumping in sapphire," Opt. Express **14**, 6366–6371 (2006).

23. P. Lassonde, F. Théberge, S. Payeur, M. Châteauneuf, J. Dubois, and J.-C. Kieffer, "Infrared generation by filamentation in air of a spectrally shaped laser beam," Opt. Express **19**, 14093–14098 (2011).

24. M. Vengris, N. Garejev, G. Tamošauskas, A. Čepėnas, L. Rimkus, A. Varanavičius, V. Jukna, and A. Dubietis, "Supercontinuum generation by co-filamentation of two color femtosecond laser pulses," Sci. Rep. **9**, 9011 (2019).

25. T. R. Ensley, D. A. Fishman, S. Webster, L. A. Padilha, D. J. Hagan, and E. W. Van Stryland, "Energy and spectral enhancement of femtosecond supercontinuum in a noble gas using a weak seed," Opt. Express **19**, 757–763 (2011).

26. C. Shanor, T. Ensley, D. J. Hagan, E. W. Van Stryland, E. M. Wright, and M. Kolesik, "Numerical investigation of enhanced femtosecond supercontinuum via a weak seed in noble gases," Opt. Express **24**, 15110–15119 (2016).

27. P. Béjot, G. Karras, F. Billard, J. Doussot, E. Hertz, B. Lavorel, and O. Faucher, "Subcycle engineering of laser filamentation in gas by harmonic seeding," Phys. Rev. A **92**, 053417 (2015).

28. J. A. Fülöp, S. Tzortzakis, and T. Kampfrath, "Laser-driven strong-field terahertz sources," Adv. Opt. Mater. **8**, 1900681 (2020).

29. Y. E, L. Zhang, A. Tcypkin, S. Kozlov, C. Zhang, and X.-C. Zhang, "Broadband THz sources from gases to liquids," Ultrafast Sci. **2021**, 1–17 (2021).

30. D. Ma, L. Dong, M. Zhang, T. Wu, Y. Zhao, L. Zhang, and C. Zhang, "Enhancement of terahertz waves from two-color laser-field induced air plasma excited using a third-color femtosecond laser," Opt. Express **28**, 20598–20608 (2020).

31. P. Salén, M. Basini, S. Bonetti, J. Hebling, M. Krasilnikov, A. Y. Nikitin, G. Shamuilov, Z. Tibai, V. Zhaunerchyk, and V. Goryashko, "Matter manipulation with extreme terahertz light: Progress in the enabling THz technology," Phys. Rep. **836–837**, 1–74 (2019).

32. V. Y. Fedorov and S. Tzortzakis, "Optimal wavelength for two-color filamentation-induced terahertz sources," Opt. Express **26**, 31150–31159 (2018).

33. R. Flender, A. Borzsonyi, and V. Chikan, "Phase-controlled, second-harmonic-optimized terahertz pulse generation in nitrogen by infrared two-color laser pulses," J. Opt. Soc. Am. B **37**, 1838–1846 (2020).

34. A. D. Koulouklidis, C. Gollner, V. Shumakova, V. Y. Fedorov, A. Pugžlys, A. Baltuška, and S. Tzortzakis, "Observation of extremely efficient terahertz generation from mid-infrared two-color laser filaments," Nat. Commun. **11**, 292 (2020).

35. A. Sukhinin, A. Aceves, and J.-C. Diels, "Two-color pulse collapse events in dispersive media," J. Opt. Soc. Am. B **36**, G62–G67 (2019).

36. X. Sun, D. Martinez, P. Froß, N. Camus, Y. Mi, W. Zhang, Z. Chen, T. Pfeifer, and R. Moshammer, "Subcycle control of the photoelectron angular distribution using two-color laser fields having different kinds of polarization," Phys. Rev. A **103**, 033106 (2021).

37. Y. Fang, C. He, M. Han, P. Ge, X. Yu, X. Ma, Y. Deng, and Y. Liu, "Strong-field ionization of Ar atoms with a 45° cross-linearly-polarized two-color laser field," Phys. Rev. A **100**, 013414 (2019).

38. N. Eicke and M. Lein, "Extracting trajectory information from two-color strong-field ionization," J. Mod. Opt. **64**, 981–986 (2017).

39. Z. Chen and F. He, "Alignment-dependent ionization of nonlinear triatomic molecules in strong laser fields," J. Opt. Soc. Am. B **36**, 2571–2578 (2019).

40. M. E. Corrales, J. González-Vázquez, G. Balerdi, I. R. Solá, R. de Nalda, and L. Bañares, "Control of ultrafast molecular photodissociation by laser-field-induced potentials," Nat. Chem. **6**, 785–790 (2014).

41. M. Kübel, M. Spanner, Z. Dube, A. Y. Naumov, S. Chelkowski, A. D. Bandrauk, M. J. J. Vrakking, P. B. Corkum, D. M. Villeneuve, and A. Staudte, "Probing multiphoton light-induced molecular potentials," Nat. Commun. **11**, 2596 (2020).

42. T. Paschen, M. Förster, M. Krüger, C. Lemell, G. Wachter, F. Libisch, T. Madlener, J. Burgdörfer, and P. Hommelhoff, "High visibility in two-color above-threshold photoemission from tungsten nanotips in a coherent control scheme," J. Mod. Opt. **64**, 1054–1060 (2017).

43. S. Kerbstadt, K. Eickhoff, T. Bayer, and M. Wollenhaupt, "Odd electron wave packets from cycloidal ultrashort laser fields," Nat. Commun. **10**, 658 (2019).

44. M. Han, P. Ge, Y. Shao, Q. Gong, and Y. Liu, "Attoclock photoelectron interferometry with two-color corotating circular fields to probe the phase and the amplitude of emitting wave packets," Phys. Rev. Lett. **120**, 073202 (2018).

45. S. D. Khosravi, M. Scipioni, and G. N. Gibson, "Toward an ultrafast double-pulse stretcher–compressor," J. Mod. Opt. **67**, 1469–1478 (2020).

46. X. Gong, C. Lin, F. He, Q. Song, K. Lin, Q. Ji, W. Zhang, J. Ma, P. Lu, Y. Liu, H. Zeng, W. Yang, and J. Wu, "Energy-resolved ultrashort delays of photoelectron emission clocked by orthogonal two-color laser fields," Phys. Rev. Lett. **118**, 143203 (2017).

47. X. Zhang, Q. Lu, Z. Zhang, Z. Fan, D. Zhou, Q. Liang, L. Yuan, S. Zhuang, K. Dorfman, and Y. Liu, "Coherent control of the multiple wavelength lasing of N2+: coherence transfer and beyond," Optica **8**, 668–673 (2021).

48. R. Trebino, *Frequency-Resolved Optical Gating: The Measurement of Ultrashort Laser Pulses*, 2000th ed. (Springer, 2002).

49. D. Keusters, H.-S. Tan, P. O'Shea, E. Zeek, R. Trebino, and W. S. Warren, "Relative-phase ambiguities in measurements of ultrashort pulses with well-separated multiple frequency components," J. Opt. Soc. Am. B **20**, 2226–2236 (2003).

50. K. W. De Long, D. N. Fittinghoff, R. Trebino, B. Kohler, and K. Wilson, "Pulse retrieval in frequency-resolved optical gating based on the method of generalized projections," Opt. Lett. **19**, 2152–2154 (1994).

51. R. Trebino, R. Jafari, S. A. Akturk, P. Bowlan, Z. Guang, P. Zhu, E. Escoto, and G. Steinmeyer, "Highly reliable measurement of ultrashort laser pulses," J. Appl. Phys. **128**, 171103 (2020).

52. L. Xu, E. Zeek, and R. Trebino, "Simulations of frequency-resolved optical gating for measuring very complex pulses," J. Opt. Soc. Am. B **25**, A70–A80 (2008).

53. R. Jafari, T. Jones, and R. Trebino, "100% reliable algorithm for second-harmonic-generation frequency-resolved optical gating," Opt. Express **27**, 2112–2124 (2019).

54. R. Jafari and R. Trebino, "Highly reliable frequency-resolved optical gating pulse-retrieval algorithmic approach," IEEE J. Quantum Electron. **55**, 1–7 (2019).

55. R. Jafari and R. Trebino, "Extremely robust pulse retrieval from even noisy second-harmonic-generation frequency-resolved optical gating traces," IEEE J. Quantum Electron. **56**, 8600108 (2020).

56. C. W. Siders, J. L. W. Siders, F. G. Omenetto, and A. J. Taylor, "Multipulse interferometric frequency-resolved optical gating," IEEE J. Quantum Electron. **35**, 432–440 (1999).

57. R. Jafari and R. Trebino, "High-speed "multi-grid" pulse-retrieval algorithm for frequency-resolved optical gating," Opt. Express **26**, 2643–2649 (2018).

58. V. Voropaev, D. Batov, A. Voronets, D. Vlasov, R. Jafari, A. Donodin, M. Tarabrin, R. Trebino, and V. Lazarev, "All-fiber ultrafast amplifier at 1.9 μm based on thulium-doped normal dispersion fiber and LMA fiber compressor," Sci. Rep. **11**, 23693 (2021).

59. R. Trebino, K. W. Delong, D. N. Fittinghoff, J. N. Sweetser, M. A. Krumbügel, B. A. Richman, and D. J. Kane, "Measuring ultrashort laser pulses in the time-frequency domain using frequency-resolved optical gating," Rev. Sci. Instrum. **68**, 3277–3295 (1997).